

Article

Development of a Ready-to-Use-Type RNA Vaccine Carrier Based on an Intracellular Environment-Responsive Lipid-like Material with Immune-Activating Vitamin E Scaffolds

Jessica Anindita ^{1,2,†}, Hiroki Tanaka ^{2,*,†}, Ryotaro Oyama ^{1,2}, Shinya Hagiwara ¹, Daiki Shirane ¹, Sakura Taneichi ³, Yuta Nakai ³, Kota Tange ³, Hiroto Hatakeyama ¹, Yu Sakurai ² and Hidetaka Akita ^{2,*}

¹ Laboratory of DDS Design and Drug Disposition, Graduate School of Pharmaceutical Sciences, Chiba University, 1-8-1 Inohana, Chuo-ku, Chiba 260-0856, Japan

² Laboratory of DDS Design and Drug Disposition, Graduate School of Pharmaceutical Sciences, Tohoku University, 6-3 Aoba, Aramaki, Aoba-ku, Sendai 980-8578, Japan

³ Life Science Research Laboratory, NOF CORPORATION, 3-3 Chidori-cho, Kawasaki-ku, Kawasaki 210-0865, Japan

* Correspondence: hiroki.tanaka.e1@tohoku.ac.jp (H.T.); hidetaka.akita.a4@tohoku.ac.jp (H.A.); Tel.: +81-22-795-6831 (H.T.); +81-22-795-6831 (H.A.)

† These authors contributed equally to this work.

Abstract: Because of its efficient and robust gene transfer capability, messenger RNA (mRNA) has become a promising tool in various research fields. The lipid nanoparticle (LNP) is considered to be a fundamental technology for an mRNA delivery system and has been used extensively for the development of RNA vaccines against SARS-CoV-2. We recently developed ssPalm, an environmentally responsive lipid-like material, as a component of LNP for mRNA delivery. In this study, a self-degradable unit (phenyl ester) that confers high transfection activity and an immune stimulating unit (vitamin E scaffold) for high immune activation were combined to design a material, namely, ssPalmE-Phe-P4C2, for vaccine use. To design a simple and user-friendly form of an RNA vaccine based on this material, a freeze-drying-based preparation method for producing a ready-to-use-type LNP (LNP(RtoU)) was used to prepare the LNP_{ssPalmE-Phe}. The optimization of the preparation method and the lipid composition of the LNP_{ssPalmE-Phe}(RtoU) revealed that dioleoyl-sn-glycero phosphatidylethanolamine (DOPE) was a suitable helper lipid for achieving a high vaccination activity of the LNP_{ssPalmE-Phe}(RtoU). Other findings indicated that to maintain particle properties and vaccination activity, a 40% cholesterol content was necessary. A single administration of the LNP_{ssPalmE-Phe}(RtoU) that contained mRNA-encoding Ovalbumin (mOVA-LNP_{ssPalmE-Phe}(RtoU)) demonstrated a significant suppression of tumor progression in a tumor-bearing mouse OVA-expressing cell line (E.G7-OVA). In summary, the LNP_{ssPalmE-Phe}(RtoU) is an easy-to-handle drug delivery system (DDS) for delivering mRNA antigens in immunotherapy.

Keywords: lipid nanoparticle; freeze-drying; mRNA vaccine



Citation: Anindita, J.; Tanaka, H.; Oyama, R.; Hagiwara, S.; Shirane, D.; Taneichi, S.; Nakai, Y.; Tange, K.; Hatakeyama, H.; Sakurai, Y.; et al. Development of a Ready-to-Use-Type RNA Vaccine Carrier Based on an Intracellular Environment-Responsive Lipid-like Material with Immune-Activating Vitamin E Scaffolds. *Pharmaceutics* **2023**, *15*, 2702. <https://doi.org/10.3390/pharmaceutics15122702>

Academic Editor: Gabriele Grassi

Received: 17 October 2023

Revised: 20 November 2023

Accepted: 27 November 2023

Published: 29 November 2023



Copyright: © 2023 by the authors. Licensee MDPI, Basel, Switzerland. This article is an open access article distributed under the terms and conditions of the Creative Commons Attribution (CC BY) license (<https://creativecommons.org/licenses/by/4.0/>).

1. Introduction

Nucleic-acid-based vaccines are based on the use of plasmid DNA (pDNA) or messenger RNA (mRNA) as a source of antigens. Upon the administration of such a vaccine, these genetic materials need to be delivered into the nucleus/cytoplasm, their site of action, where they will be transcribed/translated into antigen proteins. Since the mRNA can function in the cytoplasm and nuclear localization is not required, the mRNA can provide efficient and robust gene transfer, even in non-dividing cells [1–3]. On the other hand, since mRNA is highly susceptible to enzymatic degradation in extracellular fluid, the development of suitable delivery technology is a prerequisite for its clinical application [3,4]. One of the more promising carriers for RNA delivery is lipid nanoparticles (LNPs), which

contain an ionizable lipid as the main component. In 2018, ONPATRO® (Alnylam Pharmaceutical, Cambridge, MA, USA), an LNP-based therapeutic using small interfering RNA (siRNA), became the first ever approved RNA interference (RNAi) therapeutic for the treatment of hereditary transthyretin-mediated amyloidosis [5–9]. Moreover, the approval of RNA vaccines (mRNA-LNPs) against severe acute respiratory syndrome coronavirus 2 (SARS-CoV-2) [10–14] further demonstrated the versatility of the LNP as an mRNA carrier.

We have been developing LNPs that are composed of a series of ionizable lipids, referred to as SS-cleavable and pH-activated lipid-like materials (ssPalm). The ssPalm(s) respond to the difference in extracellular and intracellular environments based on their dual-sensing motifs: tertiary amines and a disulfide bond. After cellular uptake, the neutrally charged LNPs_{ssPalm} are sorted into endosomes. When arriving in the endosome, the LNPs are exposed to the acidic environment in the endosomal compartment (pH 6.5–5.5) and develop positive charges on their surface through the protonation of tertiary amines. The positively charged LNPs then cause endosomal membrane disruption/destabilization, which results in the endosomal escape of their cargo. Following this endosomal escape event, the disulfide bond in LNPs_{ssPalm} will be cleaved by glutathione in the reductive environment of the cytoplasm. This then triggers the decapsulation of the mRNA cargoes, releasing them into the cytoplasm [15–17].

As additional modifications of the ionizable lipids, we have focused on the hydrophobic scaffold and the linker between the amine and the scaffolds. Derivatives of ssPalms can be developed by changing their hydrophobic scaffolds. Changing the hydrophobic scaffolds from fatty acids such as myristic acid (ssPalmM) to retinoic acid (vitamin A; ssPalmA) allowed the intracellular trafficking of the nucleic acid cargo to be controlled [15]. Types of ssPalm with vitamin E scaffolds (ssPalmE) have become a focus of vaccine development since they are equipped with both gene expression activity and immune activation properties [16]. The vitamin E scaffolds were assumed to be suitable for cancer vaccines because they can efficiently activate cell-mediated immunity via the type I interferon pathway [18]. In addition to the modification of hydrophobic scaffolds, the incorporation of a self-degradable phenyl ester moiety can be used to improve the gene transfer activity of the mRNA-LNP [15,17]. The cleavage of disulfide bonds by reducing agents in the cytoplasm elevates the concentration of hydrophobic thiols in the particle. Within those limited intraparticle spaces, the concentrated thiols attack the phenyl ester and trigger a nucleophilic substitution reaction. This self-degradation reaction is irreversible, leading to the more efficient collapse of particles, which further enhances the release of the nucleic acid cargo [15,17]. In this study, a phenyl ester moiety (for achieving high transfection activity) and vitamin E scaffolds (for promoting immune activation) were combined to design ssPalmE-Phe-P4C2 for RNA vaccine development.

LNPs are generally prepared using the alcohol dilution method. In this method, the lipids and nucleic acids spontaneously form a complex due to the electrostatic interactions between the positively charged amine groups and the negatively charged nucleic acids, as well as the hydrophobic interactions between the hydrophobic moieties of lipids [19]. However, we recently reported that the post-encapsulation of mRNA into a pre-formed LNP is also applicable for use in preparing an mRNA-LNP [20]. Therefore, it is possible to encapsulate a desired mRNA into an mRNA-LNP by using pre-formed ready-to-use (RtoU) types of LNPs. Since the LNP(RtoU) can be used simply by rehydration and incubation, only a typical temperature-controlling device (i.e., block incubator, water bath, or thermal cycler) is needed for use. The development of an LNP(RtoU) using ssPalmE-Phe-P4C2 (LNP_{ssPalmE-Phe}(RtoU)) would produce a convenient form of an mRNA vaccine that offers handling practicality and vaccination efficacy. In this study, we investigated the potency of ssPalmE-Phe-P4C2 as an RNA vaccine and optimized the conditions needed for the preparation of the LNP_{ssPalmE-Phe}(RtoU). The ability to induce cytotoxic T lymphocyte (CTL) activation and antitumor activity against an E.G7-OVA tumor model was also investigated.

2. Materials and Methods

2.1. Animals

C57BL/6J mice (female, 6 weeks) were purchased from Japan SLC, Inc. (Shizuoka, Japan). Protocols for the animal experiments were reviewed and approved by the Chiba University Animal Care Committee following the “Guide for Care and Use of Laboratory Animals”.

2.2. Materials

A detailed list of supplier information, including the item numbers of all the reagents used in this study, is listed in Supporting Information (Table S1). The ssPalmE-P4C2, ssPalmE-P4C2 (Product# COATSOME[®] SS-EC), 1,2-dioleoyl-*sn*-glycero-3-phosphatidylcholine (DOPC, Product# COATSOME[®] MC-8181), and 1-(Monomethoxy polyethyleneglycol2000)2,3-dimyristoylglycerol (DMG-PEG₂₀₀₀, Product# SUNBRIGHT[®] GM-020) were supplied by NOF CORPORATION (Tokyo, Japan). The 1,2-dioleoyl-*sn*-glycero-3-phosphoethanolamine (DOPE, Product# 18:1 (Δ^9 -Cis) PE (DOPE)) was purchased from Avanti[®] Polar Lipids (Alabaster, AL, USA). Cholesterol was purchased from SIGMA Aldrich (St. Louis, MO, USA). The mRNA-encoding gene (Firefly Luciferase or Ovalbumin (OVA)) was prepared through the *in vitro* transcription reaction described in the following section. The Quant-IT[™] RiboGreen[®] RNA reagent was purchased from Thermo Fisher Scientific (Waltham, MA, USA). All other reagents and chemicals were commercially available and used without further purification.

2.3. Cell Culture

Bone-marrow-derived dendritic cell (BMDC): Murine BMDCs were isolated from the femurs of C57BL/6J mice. Bone marrow cells were cultured over 6 h in Roswell Park Memorial Institute (RPMI)-1640 medium (#R8758, SIGMA Aldrich, St. Louis, MO, USA) supplemented with 10% (*v/v*) Fetal Calf Serum (FCS, #SH30910.03, Hyclone, Logan, UT, USA), 50 μ M of 2-mercaptoethanol (#21985023, Thermo Fisher Scientific, Waltham, MA, USA), 10 mM of HEPES buffer (#17557-94, nacalai tesque, Kyoto, Japan), 1 mM of sodium pyruvate (#06977-34, nacalai tesque, Kyoto, Japan), and 100 U/mL of penicillin/streptomycin (#26253-84, nacalai tesque, Kyoto, Japan). The non-adherent cells were harvested and cultured in another dish with the same medium with an additional 10 mg/mL of Recombinant Mouse GM-CSF (#415-ML-050, R&D Systems, Minneapolis, MN, USA). Non-adherent cells were further removed on Days 2 and 4. The remaining adherent cells were cultured in a fresh culture medium containing 10 mg/mL of GM-CSF. On Day 6, the non-adherent cells were used in the experiments as immature BMDCs [16].

RAW 264.7 cell: The RAW 264.7 cells, a murine macrophage cell line, were cultured in RPMI-1640 medium (#R8758, SIGMA Aldrich, St. Louis, MO, USA) supplemented with 10% (*v/v*) Fetal Bovine Serum (FBS, #10270, Gibco, New York, USA) and 100 U/mL of penicillin/streptomycin (#26253-84, nacalai tesque, Kyoto, Japan). The adherent cells were peeled from the bottom of the dish with 0.25% Trypsin/EDTA (#32777-15, nacalai tesque, Kyoto, Japan) and cultured in another dish with a fresh medium. These cells were passaged every 2 days. The cells were used in the experiments after the third cell passage.

E.G7-OVA cell: E.G7-OVA cells, a murine lymphoma cell line EL4-expressing OVA, were purchased from the American Type Culture Collection (Manassas, VA, USA). E.G7-OVA cells were cultured in RPMI-1640 medium (#R8758, SIGMA Aldrich, St. Louis, MO, USA) supplemented with 10% (*v/v*) FCS (#SH30910.03, Hyclone, Logan, UT, USA), 50 μ M of 2-mercaptoethanol (#21985023, Thermo Fisher Scientific, Waltham, MA, USA), 10 mM of HEPES buffer (#17557-94, nacalai tesque, Kyoto, Japan), 1 mM of sodium pyruvate (#06977-34, nacalai tesque, Kyoto, Japan), 400 μ g/mL of G418 Sulfate (#074-05963, FUJIFILM Wako Pure Chemical Corporation, Tokyo, Japan), and 100 U/mL of penicillin/streptomycin (#26253-84, nacalai tesque, Kyoto, Japan). The cells were collected and cultured in another dish with a fresh medium every 2 days (cell passage). The cells were used in the experiments after the third cell passage [16].

2.4. *In Vitro* mRNA Transcription (IVT-mRNA)

The pcDNA3.1 vector was used as a coding template for Luciferase (Luc) and ovalbumin (OVA). The pcDNA3.1-Luc or pcDNA3.1-OVA were linearized with the restriction enzymes BspEI (#R0540S, New England Biolabs, Ipswich, MA, USA) or XhoI (#R0146S, New England Biolabs, Ipswich, MA, USA), respectively. After phenol-chloroform extraction and ethanol precipitation, the linearized pDNA was transcribed into mRNA with a mMESSAGE mMACHINE T7 ULTRA Transcription kit (#AM1345, Invitrogen, Waltham, MA, USA) following the manufacturer's instructions. The transcribed mRNA was dissolved in THE RNA Storage Solution (#AM7000, Invitrogen, Waltham, MA, USA) and stored at $-80\text{ }^{\circ}\text{C}$. The concentrations of linearized pDNA and transcribed mRNA were measured with a microvolume UV-Vis spectrometer (NanoDrop™ One, Thermo Fisher Scientific, Waltham, MA, USA).

2.5. Preparation of Microfluidic LNPs_{ssPalm}

The lipid composition was ssPalmE-P4C2 (or ssPalmE-Phe-P4C2)/DOPE (or DOPC)/Chol = 60/30/10 with additional DMG-PEG₂₀₀₀ (3 mol% of total lipid). The total lipid amount was 394.5 nmol to encapsulate 3 μg of mRNA (lipid/mRNA: 131.5 nmol/ μg). The lipid mixtures were dissolved in 99.5% ethanol to a concentration of 1.32 mM. The mLuc or mOVA were diluted in 20 mM of Malic acid buffer (30 mM NaCl, pH 3.0) to a concentration of 0.0033 $\mu\text{g}/\mu\text{L}$. The lipid mixtures in the ethanol and mRNA solutions were set to their respective syringes in the NanoAssemblr™ Benchtop device (Precision Nanosystems, Vancouver, Canada) with the settings of flow rate = 2.5 mL/min, flow rate ratio (buffer:lipid) = 3:1, and total volume = 1.5 mL. The LNPs were recovered and diluted with 20 mM of MES buffer (pH 5.5). The external solution of the LNPs was replaced with D-PBS (–) through ultrafiltration using Amicon Ultra-4-100K Centrifugal Units (#UFC810096, #UFC910096, Merck, Rahway, NJ, USA). The LNPs were then diluted to an adequate volume with D-PBS (–).

2.6. Preparation of LNPs_{ssPalmE-Phe} (RtoU)

The lipid composition was ssPalmE-Phe-P4C2/DOPE (or DOPC)/Chol = 52.5/7.5/40 with additional DMG-PEG₂₀₀₀ (3 mol% of total lipid) [17]. The amount of total lipid was 100 nmol, encapsulating 0.5 μg of mRNA (lipid/mRNA: 200 nmol/ μg). The lipid mixtures were dissolved in 90% t-butanol to a concentration of 8.0 mM. The lipid mixtures in t-butanol and buffer solution, containing 40 mM MES buffer (pH 5.0, salt-free) with a 744 mg/mL solution of sucrose (in equal volume), were set to their respective syringes in the NanoAssemblr™ Benchtop device (Precision Nanosystems, Vancouver, Canada) with the settings of flow rate = 1.0 mL/min, flow rate ratio (buffer:lipid) = 3:1, and total volume = 0.52 mL. An equal volume of 320 mg/mL of sucrose solution (#30404-45, nacalai tesque, Kyoto, Japan) was added (final concentration of sucrose in the LNP solution = 320 mg/mL). The LNP solution was frozen in liquid nitrogen and transferred to the freeze-dryer (FDU-2110, EYELA, Tokyo, Japan). The drying sequence of the freeze-dryer was set to 9 segments: $-40\text{ }^{\circ}\text{C}$ ($\pm 7\text{ }^{\circ}\text{C}$, 40 min), $-40\text{ }^{\circ}\text{C}$ (vacuum start, 20 min), $-30\text{ }^{\circ}\text{C}$ (1 h), $-20\text{ }^{\circ}\text{C}$ (1 h), $-10\text{ }^{\circ}\text{C}$ (1 h), $0\text{ }^{\circ}\text{C}$ (1 h), $10\text{ }^{\circ}\text{C}$ (1 h), $20\text{ }^{\circ}\text{C}$ (1 h), and $30\text{ }^{\circ}\text{C}$ (3 h). The freeze-dried LNPs were recovered, and their physical appearances were inspected for visible cracks, dents, or collapses in front of a black background [21]. The dry LNPs were reconstituted with a water solution containing 0.5 μg of either mLuc or mOVA (0.0025 $\mu\text{g}/\mu\text{L}$). The solution was mixed well, followed by heating at $95\text{ }^{\circ}\text{C}$ for 5 min, then allowed to cool to room temperature (RT) for approximately 10 min before use in the experiments/analysis.

2.7. Characterization of mRNA-LNPs

The particle size, polydispersity index (PdI), and zeta-potential of the LNPs were measured via dynamic light scattering (Zetasizer Nano ZS, Malvern Panalytical, Malvern, UK). The recovery ratio and encapsulation efficiency of the mRNA were evaluated with RiboGreen® assay. Solutions containing Quant-iT™ RiboGreen® RNA reagent (#R11491, Invitrogen, Waltham, MA, USA) with or without 10% (*v/v*) TritonX-100 (#168-11805, FU-

JIFILM Wako Pure Chemical Corporation, Tokyo, Japan), in respective 1:8 ratios were prepared in D-PBS (–): Triton [+] (contained both RiboGreen[®] and TritonX-100) and Triton [–] (no TritonX-100, only RiboGreen[®]). The mRNA-LNPs, corresponding to 50 ng of mRNA in 50 µL of D-PBS (–), were prepared twice and each mixed with an equal volume of the Triton [+] and Triton [–] solution in a 96-well black microplate. A calibration curve was prepared through sequential dilution from 0 to 2000 ng/mL of mRNA. The plate was incubated for 5 min with shaking at 500 rpm in a shaking incubator. The fluorescence intensities were analyzed with a plate reader (Infinite M200 PRO, TECAN, Männedorf, Switzerland) set with emission and excitation waves of 484 nm and 535 nm, respectively. The recovery ratio was calculated from the total mRNA (quantified by Triton [+] addition) and mRNA concentration input (standard curve). The encapsulation efficiency was calculated as the ratio of the total mRNA concentration (quantified by Triton [+] addition) to the non-encapsulated mRNA concentration (quantified by Triton [–] addition).

2.8. Evaluation of In Vitro Gene Expression Efficiency

BMDCs (8×10^5 cells/mL) and RAW 264.7 cells (2×10^5 cells/mL) seeded in a 12-well plate were transfected with mLuc-LNPs in D-PBS (–) at a dose of 0.8 µg of mRNA. In the case of RAW 264.7 cells, the transfection was demonstrated after pre-incubation for 24 h. After transfection, the BMDCs and RAW 264.7 cells were incubated at 37 °C with 5% CO₂ for 5 h. The BMDCs and RAW 264.7 cell suspensions were collected, washed with D-PBS (–), and then solubilized with Reporter Lysis Buffer (#E397A, Promega, Madison, WI, USA). The cell lysates were added with a Nano-Glo[®] Luciferase Assay System (#E1501, Promega), and the luminescence intensities were quantified with a luminometer (GloMax[®] 20/20 Luminometer, Promega, Madison, WI, USA). The protein amount in the cell lysates was determined using the Bicinchoninic acid (BCA) Protein Assay kit (#T9300A, Takara Bio Inc., Kusatsu, Shiga, Japan) according to the manufacturer's instructions. Luciferase activity was represented as a relative light unit (RLU/mg protein), calculated by dividing the luminescence intensity by the protein amount [16].

2.9. Evaluation of In Vivo Gene Expression Efficiency (IVIS Imaging)

The mLuc-LNPs in D-PBS (–) were administered subcutaneously (back of neck) to C57BL/6J mice at a dose of 1.0 µg of mRNA under anesthetized conditions. The neck region of mice was shaved in advance. Six hours later, D-Luciferin potassium (#126-05116, FUJIFILM Wako Pure Chemical Corporation, Tokyo, Japan) in D-PBS (–) (3 mg/200 µL/mouse) was administered intraperitoneally. After 30 min had passed, the luminescence intensities were measured with an In Vivo Imaging System (IVIS[®] Lumina II, Caliper Life Sciences, Waltham, MA, USA).

2.10. In Vivo Cytotoxic T Lymphocyte (CTL) Assay

The in vivo CTL assay was performed as described previously [16]. The mOVA-LNPs in D-PBS (–) were injected subcutaneously (back of neck) to C57BL/6J mice at a dose of 0.05 or 0.1 µg of mRNA under anesthetized conditions. Seven days after the LNP administration (immunization), the non-treated (NT) mice were sacrificed, and their spleens were collected into a dish containing RPMI-1640 medium (#R8758, SIGMA Aldrich, St. Louis, MO, USA) supplemented with 10% (*v/v*) FCS (#SH30910.03, Hyclone, Logan, UT, USA), 50 µM of 2-mercaptoethanol (#21985023, Thermo Fisher Scientific, Waltham, MA, USA), 10 mM of HEPES buffer (#17557-94, nacalai tesque, Kyoto, Japan), 1 mM of sodium pyruvate (#06977-34, nacalai tesque, Kyoto, Japan), and 100 U/mL of penicillin/streptomycin (#26253-84, nacalai tesque, Kyoto, Japan). The cell suspension of the splenocytes was filtered through a 40 µm cell strainer and resuspended in Red Blood Cell Lysing Buffer (#R7757-100ML, SIGMA Aldrich, St. Louis, MO, USA). The cell suspension was washed and resuspended in a fresh medium, then equally divided into two suspensions: CFSE^{high}- and CFSE^{low}-labelled. Each cell suspension was resuspended in a 1.0×10^7 cells/mL cell concentration. The OVA H-2K^b cytotoxic T-lymphocyte epitope peptide (SIINFEKL, OVA_{257–264}) in DMSO

was added to the CFSE^{high}-labelled cells (1/400 of the suspension volume). Both cell suspensions were incubated at 37 °C with 5% CO₂ for 1 h. Each cell suspension was adjusted to a 3.0×10^7 cells/mL cell concentration in D-PBS (–). The CFSE^{high} (5.0 μM) and CFSE^{low} (0.5 μM) (Cellstain CFSE, #C375, Dojindo Laboratories, Kumamoto, Japan) cells were added to their respective cell suspension tubes and incubated in a 37 °C water bath for 10 min under a light-shielding condition. Each cell suspension was washed repeatedly with a fresh medium and D-PBS (–), then resuspended in 5.0×10^7 cells/mL cell concentration in D-PBS (–). The cells were administered intravenously into the immunized mice with equal volumes (ratio 1:1) of CFSE^{high}- and CFSE^{low}-labelled splenocytes. Twenty hours after administration, the spleens were collected from the immunized mice, and the splenocytes were suspended into single-cell suspensions in FACS buffer (0.5% Bovine Serum Albumin (#01860-07, nacalai tesque, Kyoto, Japan) and 0.1% NaN₃ (#194-01275, FUJIFILM Wako Pure Chemical Corporation, Tokyo, Japan) in D-PBS (–)). The number of CFSE-labeled cells (CFSE^{high} and CFSE^{low}) was quantified with a flow cytometer (NovoCyt Flow Cytometer, Agilent, Santa Clara, CA, USA). The CTL activity was represented by the degree of cell lysis, calculated as the ratio of the number of CFSE^{high}-labelled cells to CFSE^{low}-labelled cells.

2.11. Therapeutic Anti-Tumor Response against E.G7-OVA

E.G7-OVA cells (8.0×10^7 cells/40 μL) suspended in D-PBS (–) were inoculated subcutaneously on the left flank of mice in anesthetized conditions. After the tumor grew to ≥ 100 mm³ (approximately after 7–9 days), the mice were injected subcutaneously (back of neck) with mOVA-LNPs (0.5 μg of mRNA) in D-PBS (–). Tumor sizes were measured at 3-day intervals with the calculation formula: {long axis} × {short axis}² × 0.52 [16]. The endpoint of tumor measurement was set to 1000 mm³.

3. Results

3.1. Transfection Efficiency and Immune Activity of LNPs

The ssPalmE-Phe-P4C2 (Figure 1a) was developed by introducing a phenyl ester moiety into ssPalmE-P4C2, a derivative of ssPalm with a vitamin E scaffold [15,17]. Helper lipids, such as 1,2-dioleoyl-*sn*-glycero-3-phosphatidylcholine (DOPC) or 1,2-dioleoyl-*sn*-glycero-3-phosphoethanolamine (DOPE), cholesterol, and 1-(Monomethoxy polyethyleneglycol2000)2,3-dimyristoylglycerol (DMG-PEG₂₀₀₀) (Figure 1a), were incorporated to stabilize the LNP formulation. To investigate the effects of the phenyl ester group that was inserted into the structure, the transfection efficiency and immune activation ability of the LNPs containing the ssPalmE-Phe-P4C2 (LNPs_{ssPalmE-Phe}) were compared with those containing the ssPalmE-P4C2 (LNPs_{ssPalmE}). The LNP_{ssPalmE-Phe}- and LNP_{ssPalmE}-containing luciferase mRNAs (mLuc-LNPs) were prepared by means of a microfluidic mixer. The composition of the LNPs was ssPalm/DOPE/Chol = 60/30/10 with an additional 3% DMG-PEG₂₀₀₀ [17]. The properties of both the mLuc-LNPs_{ssPalmE-Phe} and mLuc-LNPs_{ssPalmE} were similar, with sizes of around 70–90 nm, an acceptable polydispersity index (PDI) (<0.200), and a neutral surface charge (0 to –2 mV). Both types of LNPs had a high mRNA encapsulation rate (>90%) and comparable recovery rates (60–75%) (Figure 2a).

Both an in vitro and in vivo quantifications of gene expression were performed to evaluate the effect of the phenyl ester group on transfection efficiency. An in vitro luciferase assay was performed using bone-marrow-derived dendritic cells (BMDCs) (Figure 2b) and RAW 264.7 cells of a murine macrophage/monocyte cell line (Figure 2c). Luciferase activity was evaluated 6 h after the transfection. The mLuc-LNPs_{ssPalmE-Phe} exhibited significantly higher luciferase activity in the BMDCs compared to the mLuc-LNPs_{ssPalmE}. The gene expression of the mLuc-LNPs_{ssPalmE-Phe} in RAW 264.7 cells was also significantly higher than that of the LNPs_{ssPalmE} (Figure 2c). A similar trend was also found in the in vivo gene expression of mLuc-LNPs on the skin at the back of the neck at a dose of 1.0 μg of mRNA (Figure 2d,e).

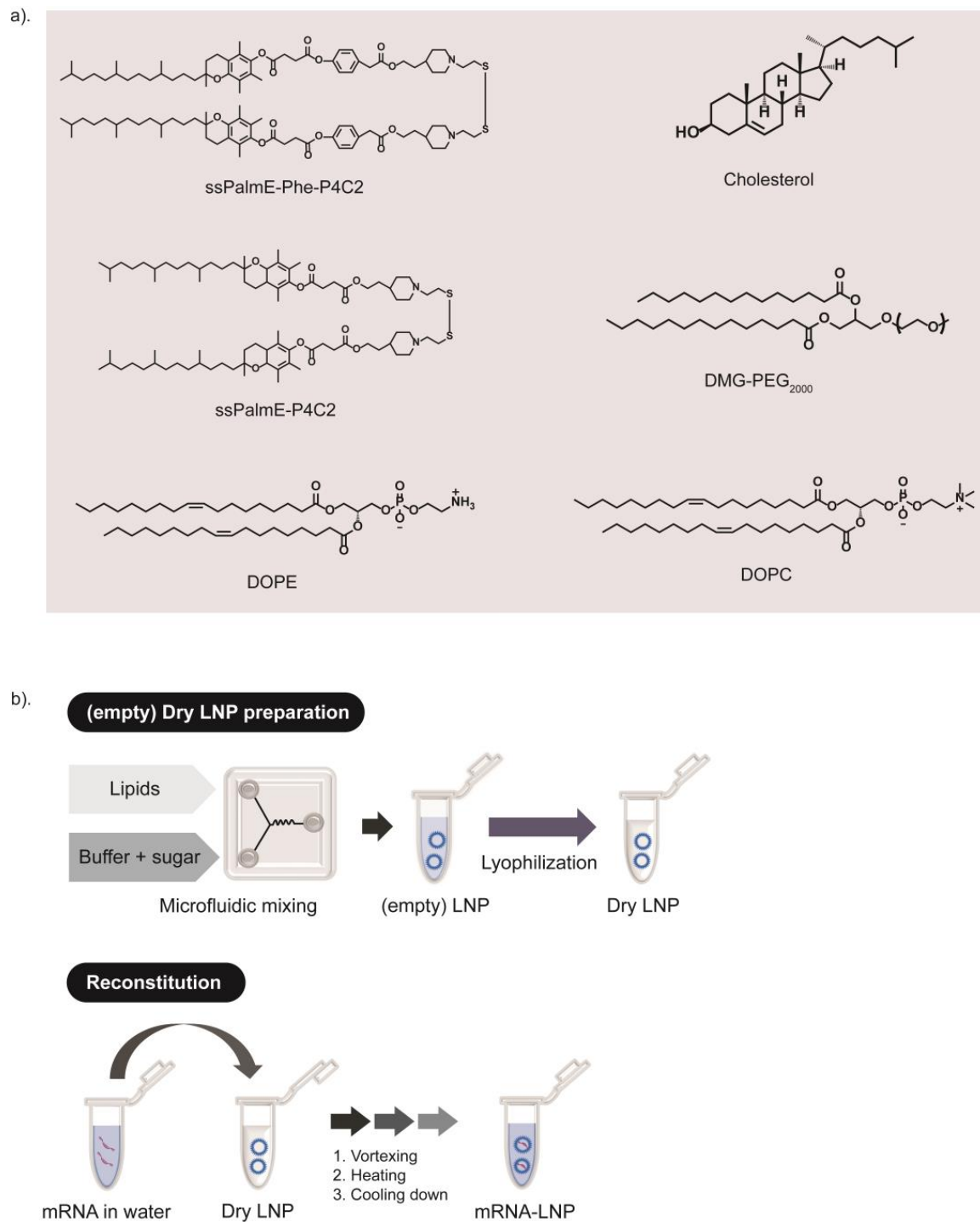


Figure 1. Chemical structure of lipid components and schematic illustration of the experimental design. (a) The molecular structures of ssPalmE-Phe-P4C2, ssPalmE-P4C2, DOPE, DOPC, cholesterol, and DMG-PEG₂₀₀₀ are shown. (b) Experimental design of LNP_{ssPalmE-Phe}(RtoU) preparation; the empty LNPs were prepared through microfluidic mixing and then lyophilized to produce dry empty LNPs. The mRNA-encapsulated LNPs could be obtained via the reconstitution (rehydration) of the dry LNPs with the mRNA solution in water.

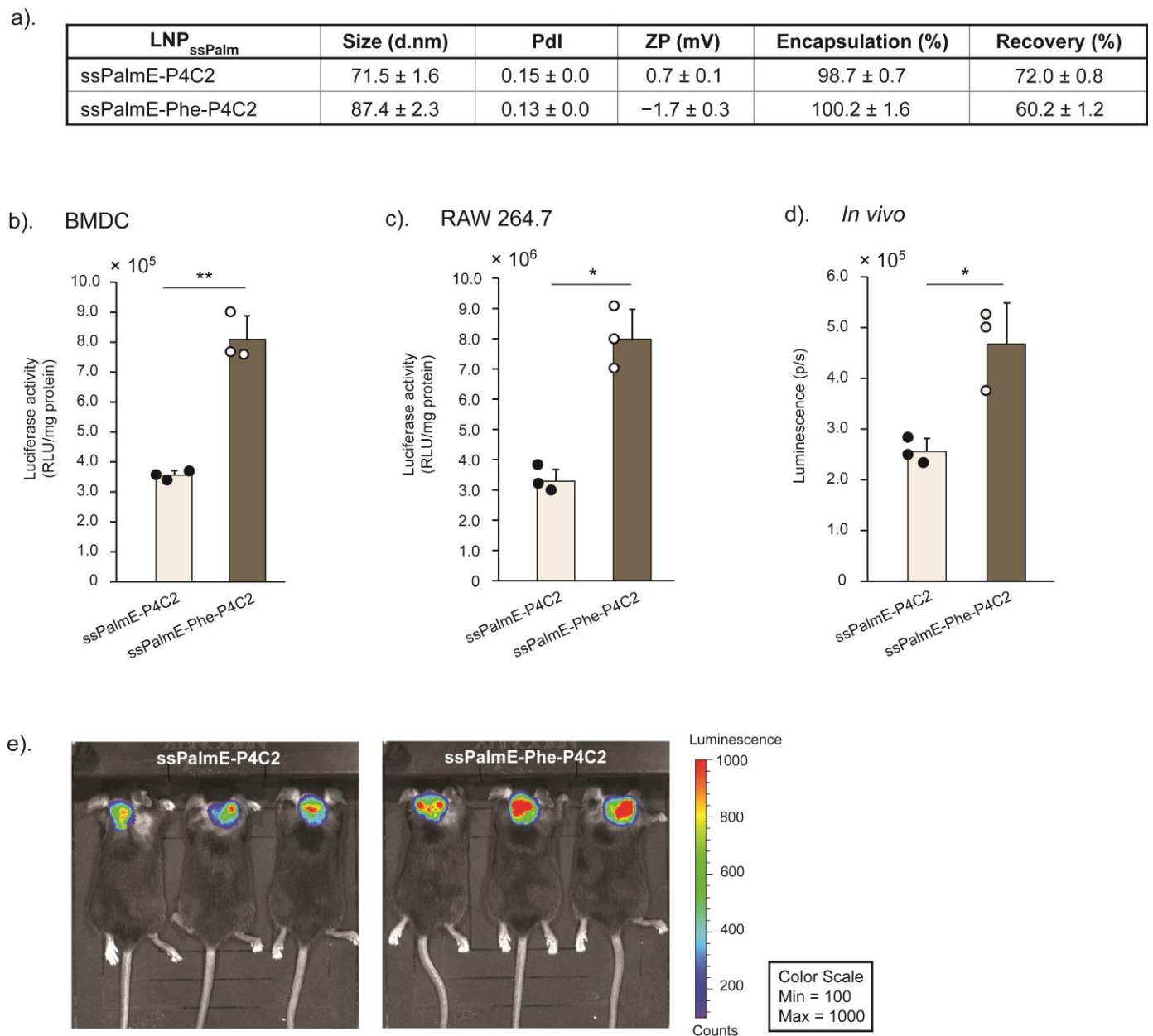


Figure 2. In vitro and in vivo gene expressions of LNP_{ssPalmE} and LNP_{ssPalmE-Phe} prepared with a microfluidic device. (a) Physicochemical properties of LNP_{ssPalmE} and LNP_{ssPalmE-Phe}. In vitro gene expression after transfection of mLuc-LNPs at a dose of 0.8 µg of mRNA in (b) BMDCs (8.0×10^5 cells) and (c) RAW 264.7 cells (2.0×10^5 cells). Luciferase activity is represented as a relative light unit (RLU/mg protein), calculated from the luminescence intensities and protein content of the cell lysates. (d,e) Quantification and imaging results of the in vivo mLuc-LNP gene expression in C57BL/6J mice through immunization (s.c.) of 1.0 µg of mRNA. Six hours after administration, D-luciferin potassium (3 mg/200 µL/mouse) was administered (i.p.), and the luminescence intensities were measured using an IVIS device. The scatter graph represents the individual value; the bar graph represents the mean with SD ($n = 3$); * $p < 0.05$; ** $p < 0.01$ (two-tail unpaired *t*-test). The measurements in the in vitro experiments were conducted in triplicate.

The ability to activate cell-mediated immunity for both the LNP_{ssPalmE-Phe} and the LNP_{ssPalmE}, with either DOPE or DOPC as helper lipids, was evaluated with a CTL assay against the model antigen ovalbumin (OVA). As shown in Figure 3, the mOVA-LNP_{ssPalmE-Phe} had an overall higher CTL activity than the mOVA-LNP_{ssPalmE}, with either

helper lipid being used. The use of DOPE as a helper lipid in the mOVA-LNP_{ssPalmE-Phe} provided the highest CTL activity (Figure 3). Collectively, the higher gene expression activity and vaccination activity of the LNP_{ssPalmE-Phe} indicated that the insertion of a phenyl ester group improved the function of the ionizable lipid with a vitamin E scaffold.

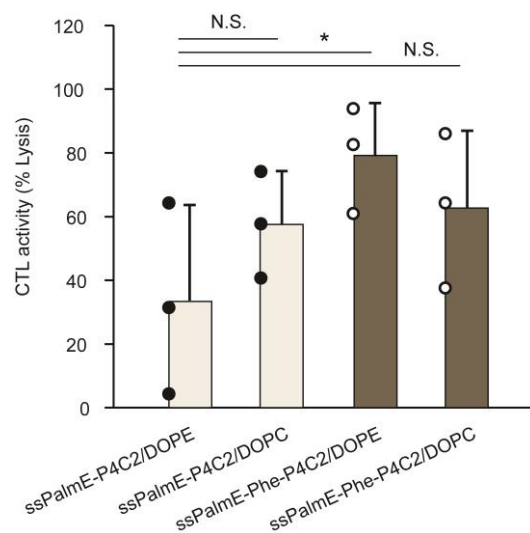


Figure 3. CTL activity of the LNP_{ssPalmE} and LNP_{ssPalmE-Phe} prepared using a microfluidic device. The mOVA-LNP_{ssPalmE} and mOVA-LNP_{ssPalmE-Phe}, with either DOPE or DOPC as helper lipids, were evaluated for their immune activation activity via a CTL assay. The CTL assays of the mOVA-LNPs were conducted in C57BL/6J mice via immunization (s.c.) of 0.05 µg of mRNA. On day 7 after immunization, the mice were injected (i.v.) with equal amounts of CFSE^{hi}-labelled splenocytes (SIINFEKL OVA epitope) and CFSE^{low}-labelled splenocytes (naïve). The spleen was collected on Day 8, and the % lysis of splenocytes was quantified via flow cytometry. The scatter graph represents individual values; the bar graph represents the mean with SD ($n = 3$). N.S.: not significant; * $p < 0.05$ (one-way ANOVA followed by the Bonferroni test against the original LNP_{ssPalmE}).

3.2. Ready-to-Use-Type RNA Vaccine Development

The preparation method for the lyophilized ready-to-use LNP formulation (LNP_{ssPalmE} (RtoU)) was then applied to the LNP_{ssPalmE-Phe} to further improve their usability. To apply the preparation method, the lipid composition was adjusted to the previously reported LNP_{ssPalmE} (RtoU) (ssPalmE/DOPC/Chol = 52.5/7.5/40 (% of total lipid)) [17,20]. We initially applied both the default RtoU composition (ssPalmE-Phe-P4C2/helper lipid/cholesterol = 52.5/7.5/40) and the microfluidic-mixer-type LNP_{ssPalmE-Phe} (ssPalmE-Phe-P4C2/helper lipid/cholesterol = 60/30/10), with a fixed DMG-PEG₂₀₀₀ ratio of 3 mol% of total lipid. Two types of helper lipids, DOPE and DOPC, were used in the lipid formulation. A stock solution of the lipids prepared in 90% *t*-butanol was prepared. The mixture of the lipids was then mixed with a 40 mM MES (pH 5.0) buffer with a NanoAssemblr device to prepare empty LNPs. An equal volume of 320 mg/mL of sucrose was then added into the empty LNP_{ssPalmE-Phe}. The LNP solution was frozen in liquid nitrogen and then transferred to the freeze-drying equipment. The recovered lyophilized empty LNP_{ssPalmE-Phe} (RtoU) can be reconstituted with the intended mRNA solution in an aqueous medium, followed by heating at 95 °C for 5 min. After cooling, the LNPs were neutralized with an equal volume of PBS and used for the following experiments/analysis (Figure 1b).

The physicochemical properties of mOVA-LNP_{ssPalmE-Phe} (RtoU) are shown in Table 1. The mOVA-LNP_{ssPalmE-Phe} (RtoU) with the ssPalmE-Phe-P4C2/helper lipid (DOPE or DOPC)/Chol = 60/30/10 formulation showed particle sizes of around 110–120 nm with a slightly high PDI (0.200–0.240) and a neutral charge (−2 mV). On the other hand, in the case of the other lipid composition, the ssPalmE-Phe-P4C2/helper lipid/Chol = 52.5/7.5/40 formulation, the particle sizes were slightly larger (120–140 nm), with an acceptable range of PDI (≤ 0.200) and a light negative charge (−10 mV). All formulations had high mRNA encap-

sulation efficiencies (>90%) after simple rehydration and incubation. The immune activation activity of the LNP_{ssPalmE-Phe}(RtoU) was compared with their ability to induce CTL activity. The reconstituted mRNA-LNP_{ssPalmE-Phe}(RtoU) were directly injected into the mice for immunization. The CTL activity was not affected by the presence or absence of ultrafiltration steps (Figure S1) for the mRNA-LNP_{ssPalmE-Phe}(RtoU). The mOVA-LNP_{ssPalmE-Phe}(RtoU) with the ssPalmE-Phe-P4C2/helper lipid (DOPE or DOPC)/Chol = 52.5/7.5/40 formulations showed an overall better induction of CTL activity (Figure 4). Moreover, the use of DOPE resulted in the highest CTL activity (Figure 4). These results indicate that the LNP_{ssPalmE-Phe}(RtoU) with a composition of ssPalm/DOPE/Chol = 52.5/7.5/40 is suitable for the development of an RNA vaccine.

Table 1. Physicochemical properties of LNP_{ssPalmE-Phe}(RtoU) with different compositions.

Composition (%)	Helper Lipid	mRNA	Size (d.nm)	PDI	ZP	Encaps.	Recovery
					(mV)	(%)	(%)
60/30/10	DOPE	empty	115.6	0.18	−1.2	-	-
60/30/10	DOPE	OVA	113.4	0.22	−2.8	94.3	83.2
60/30/10	DOPC	OVA	117.9	0.24	0.7	93.7	99.1
52.5/7.5/40	DOPE	empty	130.2	0.17	−8.3	-	-
52.5/7.5/40	DOPE	OVA	128.1	0.18	−10.7	94.3	77.0
52.5/7.5/40	DOPC	OVA	131.4	0.19	−9.2	94.3	81.7

Size, PDI, and ZP were measured with Zetasizer Nano ZS. Encapsulation efficiency was measured with Ribogreen[®] assay. Composition (%) represents the ssPalmE-Phe-P4C2/helper lipid/cholesterol ratio.

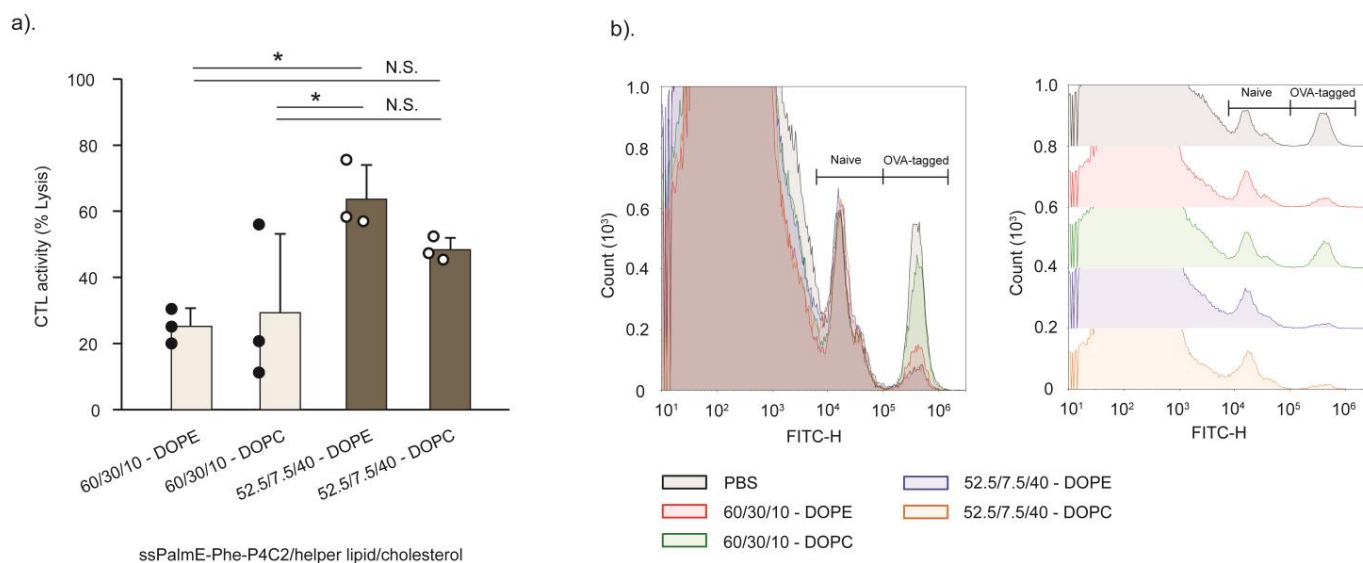


Figure 4. CTL activity of LNP_{ssPalmE-Phe}(RtoU) with different lipid compositions. (a) The activation of the antigen-specific cellular immunity of the LNP_{ssPalmE-Phe}(RtoU) with the lipid composition of ssPalmE-Phe-P4C2/(DOPE or DOPC)/cholesterol = 60/30/10 and ssPalmE-Phe-P4C2/(DOPE or DOPC)/cholesterol = 52.5/7.5/40 was evaluated via CTL assays. All lipid compositions included an additional 3 mol% of DMG-PEG₂₀₀₀. (b) The overlaid (left) and offset (right) FACS histogram from the CTL assay. CTL assays of mOVA-LNPs(RtoU) were conducted in C57BL/6J mice via immunization (s.c.) with 0.1 μg of mRNA. The spleen was collected, and the % lysis of splenocytes was quantified via flow cytometry. The scatter graph represents the individual values; the bar graph represents the mean with SD ($n = 3$). N.S.: not significant; * $p < 0.05$ (one-way ANOVA followed by SNK test).

3.3. Optimization of Buffer pH and Cryoprotectant Concentration

Concerning the preparation of the LNP_{ssPalmE-Phe}(RtoU), an acidic buffer pH is important since the cationic charge is accompanied by the protonation of the ionizable lipid, which

is plausibly a crucial driving force for the post-encapsulation of the negatively charged mRNA. In parallel, a cryoprotectant is needed to protect the LNPs from damage during the freeze-drying process [20]. The regimen for preparing the LNPs_{ssPalmE-Phe}(RtoU) was optimized by changing the pH of the 20 mM MES buffer (pH 5.00–6.00) and sucrose concentrations (80–320 mg/mL). As a first screening, the freeze-dried appearance and physicochemical properties of the mOVA-LNPs_{ssPalmE-Phe}(RtoU) after rehydration are also shown in Table 2. The appearance of the freeze-dried material was labeled as ‘good’, ‘dent’, ‘crack’, and ‘collapse’ (Figure S2) based on the literature [21,22]. The LNPs_{ssPalmE-Phe}(RtoU) that were labeled as ‘good’ or ‘dent’ were considered to have an acceptable appearance [22]. The lyophilized LNPs_{ssPalmE-Phe}(RtoU) that showed an acceptable appearance and properties were further evaluated for their capabilities to induce immune activity: LNPs_{ssPalmE-Phe}(RtoU) with a buffer of pH 5.25 had 80 mg/mL of sucrose, pH 5.25–160 mg/mL of sucrose, pH 5.50–160 mg/mL of sucrose, and pH 5.00–320 mg/mL of sucrose.

Table 2. Physicochemical properties of the LNPs_{ssPalmE-Phe}(RtoU) prepared with different buffer pH(s) and sucrose concentrations.

Sucrose (mg/mL)	Buffer pH	Size (d.nm)	PdI	ZP (mV)	Appearance	Encaps. (%)
80		167.2	0.16	−10.6	good	82.8
	*	153.7	0.10	−11.5	good	99.4
		179.8	0.17	−11.5	crack	100.7
		220.5	0.32	−12.3	crack	101.1
		303.2	0.48	−12.6	crack	100.8
160		170.2	0.14	−13.0	good	100.6
	*	169.4	0.13	−11.1	good	99.3
	*	206.6	0.22	−11.8	good	100.6
		244.2	0.34	−12.6	good	100.8
		287.9	0.40	−13.2	good	100.4
320	*	160.9	0.19	−12.9	dent	95.5
		311.1	0.26	−13.1	dent	100.2
		417.4	0.69	−13.3	dent	100.0
		313.2	0.42	−14.3	dent	100.4
		1158.0	0.79	−14.5	dent	98.3

Size, PdI, and ZP were measured with Zetasizer Nano ZS. Encapsulation efficiency was measured with Ribogreen[®] assay. The samples with asterisks (*) were evaluated for CTL activity.

As a result, the LNPs_{ssPalmE-Phe}(RtoU) prepared with a buffer pH of 5.00 and 320 mg/mL of sucrose exhibited the highest CTL activity among the other groups and was comparable with those with a buffer pH of 5.50 and a sucrose concentration of 160 mg/mL (Figure 5). The lyophilized appearance of the LNPs_{ssPalmE-Phe}(RtoU) with a buffer with a pH of 5.00 and a sucrose concentration of 320 mg/mL (dent) appeared to be not as good as those with a buffer pH of 5.50 and a sucrose concentration of 160 mg/mL (good). However, the particle size and PdI of the LNPs_{ssPalmE-Phe}(RtoU) with a buffer pH of 5.00 and a sucrose concentration of 320 mg/mL were better (Table 2). This indicated that the ‘dent’ appearance might have negligible effects on the properties of the LNPs_{ssPalmE-Phe}(RtoU) after hydration with mRNA. Based on these results, we concluded that the optimal buffer and sucrose concentrations for preparing the LNPs_{ssPalmE-Phe}(RtoU) were 20 mM of MES buffer (pH 5.00) and 320 mg/mL of sucrose, respectively.

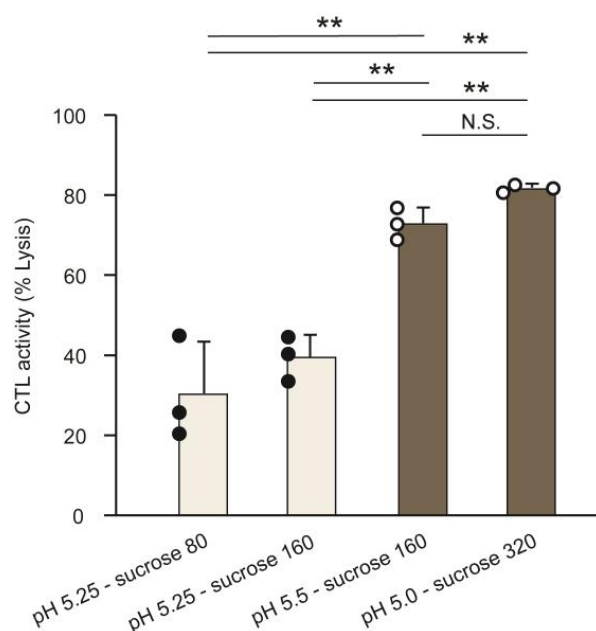


Figure 5. CTL activity of LNP_{ssPalmE-Phe}(RtoU) prepared using different buffer pHs and sucrose concentrations. The CTL activity for combined buffer pH(s) and sucrose concentrations was evaluated and exhibited acceptable appearances and physicochemical properties, as shown in Table 2. A CTL assay of mOVA-LNPs(RtoU) was conducted in C57BL/6J mice via immunization (s.c.) with 0.1 µg of mRNA. The spleen was collected, and the % lysis of splenocytes was quantified via flow cytometry. The scatter graph represents individual values; the bar graph represents the mean with SD ($n = 3$). N.S.: not significant; ** $p < 0.01$ (one-way ANOVA followed by SNK test).

3.4. Lipid Composition Screening

To investigate the issue of whether the ssPalm-Phe-P4C2/DOPE/Chol = 52.5/7.5/40 composition was optimal for LNP_{ssPalmE-Phe}(RtoU), a screening of the lipid composition was further conducted using a total of 24 lipid compositions with various cholesterol and DOPE ratios (Table S2) through CTL assays. All formulations produced mRNA-LNP_{ssPalmE-Phe}(RtoU) with sizes ranging from 160 to 230 nm, PdIs ranging from 0.150 to 0.240, acceptable appearances (dent), encapsulation efficiencies $\geq 90\%$, and recovery rates $\geq 80\%$. The mRNA-LNP_{ssPalmE-Phe}(RtoU) with the ssPalmE-Phe-P4C2/DOPE/Chol = 52.5/7.5/40 formulation were used as a control in each evaluation. Within the same cholesterol ratio, the CTL activities were maintained or tended to increase with a reduction in the DOPE ratio (Figures 6a and S3a–c). Thus, a lipid composition with a lower DOPE density was evaluated.

In the LNP_{ssPalmE-Phe}(RtoU) with 40% Chol, the optimal range of DOPE was narrow (5–10%): the CTL activity increased when the DOPE ratio was 0–5% but then slightly decreased when the density of DOPE reached 7.5% (Figure 6b). Meanwhile, for the LNP_{ssPalmE-Phe}(RtoU) with 50% Chol, the CTL activity increased when the DOPE ratio was 0–7.5% and then sharply decreased with a DOPE ratio above 10% (Figure 6c). Similarly, the optimal DOPE ratio was also narrow (5–10% DOPE).

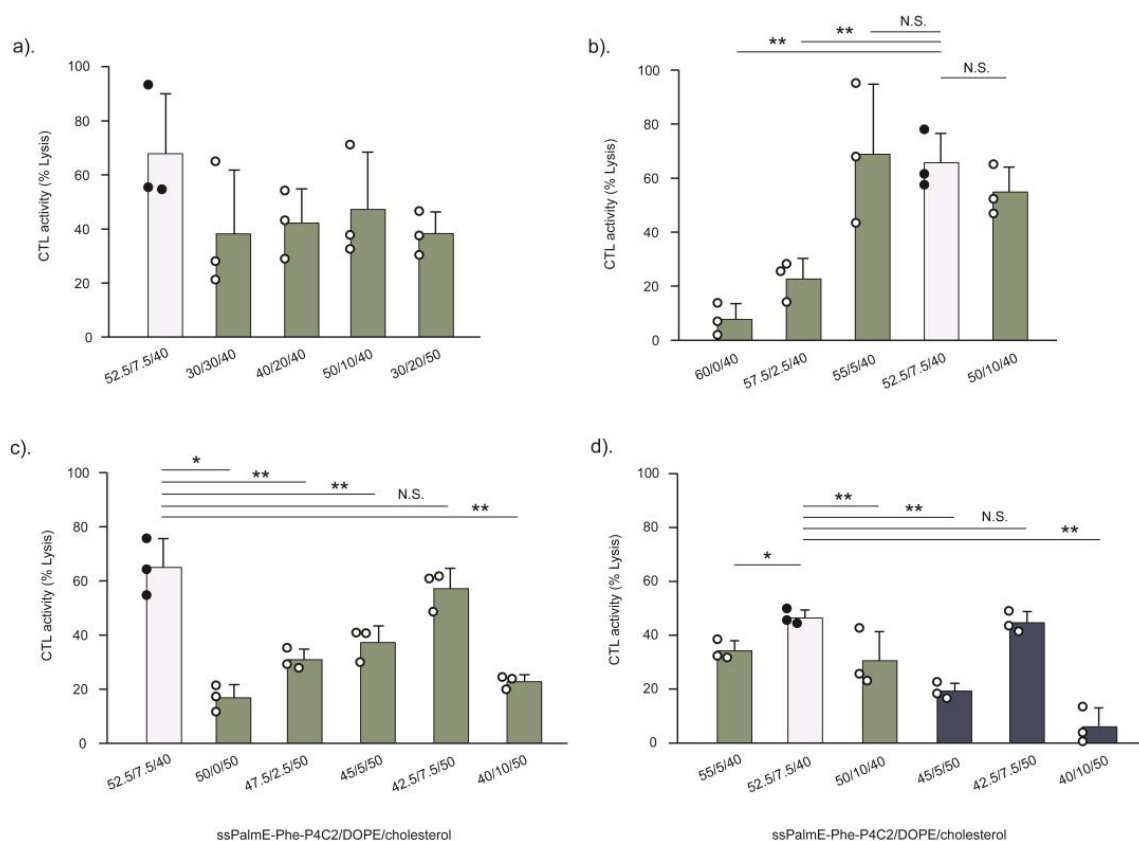


Figure 6. CTL activity evaluation of LNPs_{ssPalmE-Phe}(RtoU) prepared using various lipid compositions. The LNPs_{ssPalmE-Phe}(RtoU) were prepared with a total of 24 lipid compositions (Table S2), and their immune activation activities were evaluated via CTL assays at a dose of 0.1 µg of mRNA. (a) CTL activity of LNPs_{ssPalmE-Phe}(RtoU) with 40% Chol. (b) CTL activity of LNPs_{ssPalmE-Phe}(RtoU) with 0–10% DOPE (with 40% Chol). (c) CTL activity of LNPs_{ssPalmE-Phe}(RtoU) with 0–10% DOPE (with 50% Chol). (d) CTL activity of LNPs_{ssPalmE-Phe}(RtoU) with a DOPE ratio of 5–10% and 40 or 50% Chol. The lipid composition of ssPalmE-Phe-P4C2/DOPE/Chol = 52.5/7.5/40 was still found to be the favorable formulation for LNPs_{ssPalmE-Phe}(RtoU). The scatter graph represents individual values; the bar graph represents the mean with SD ($n = 3$); white bar: control group; N.S.: not significant; * $p < 0.05$; ** $p < 0.01$ (one-way ANOVA followed by Bonferroni testing against the control group). There were no significant differences found in all groups (against control group) in Figure 6a.

Finally, the CTL activities of the LNPs_{ssPalmE-Phe}(RtoU) with 5–10% DOPE and 40 or 50% Chol were compared. The LNPs_{ssPalmE-Phe}(RtoU) with 50% Chol and a DOPE ratio of 7.5% showed comparable CTL activity with those with 40% Chol and a DOPE ratio of 7.5% (control) (Figure 6d). However, the CTL activity of the LNPs_{ssPalmE-Phe}(RtoU) with 50% Chol was more sensitive to the content of DOPE (Figure 6d). This drastic loss in CTL activity depending on the DOPE density is not desirable when considering batch-to-batch reproducibility. We therefore concluded that the initial formulation of ssPalmE-Phe-P4C2/DOPE/Chol = 52.5/7.5/40 was the most favorable lipid composition for LNPs_{ssPalmE-Phe}(RtoU) from the viewpoint of CTL activity and physicochemical properties: with a particle size of 158.9 ± 0.4 nm, a PDI of 0.19 ± 7.8 , a dented freeze-dried appearance, a $100 \pm 2.3\%$ encapsulation efficiency, and a $102.1 \pm 7.1\%$ recovery rate.

3.5. Therapeutic Anti-Tumor Response against E.G7-OVA Tumor Model

To determine the capability of the LNPs_{ssPalmE-Phe}(RtoU) to function as an mRNA-based vaccine carrier, its therapeutic anti-tumor response against an E.G7-OVA (murine-thymus-lymphoma-expressing ovalbumin) tumor model was evaluated. A subcutaneous administra-

tion (a single dose of 0.5 μg of mRNA) significantly suppressed tumor progression. Moreover, the survival analysis indicated that the immunized mice completely survived until 30 days after the tumor inoculation, when the endpoint was set at a 1000 mm^3 tumor size (Figure 7). Collectively, $\text{LNPs}_{\text{ssPalmE-Phe}}(\text{RtoU})$ can be a potent mRNA-based vaccine carrier.

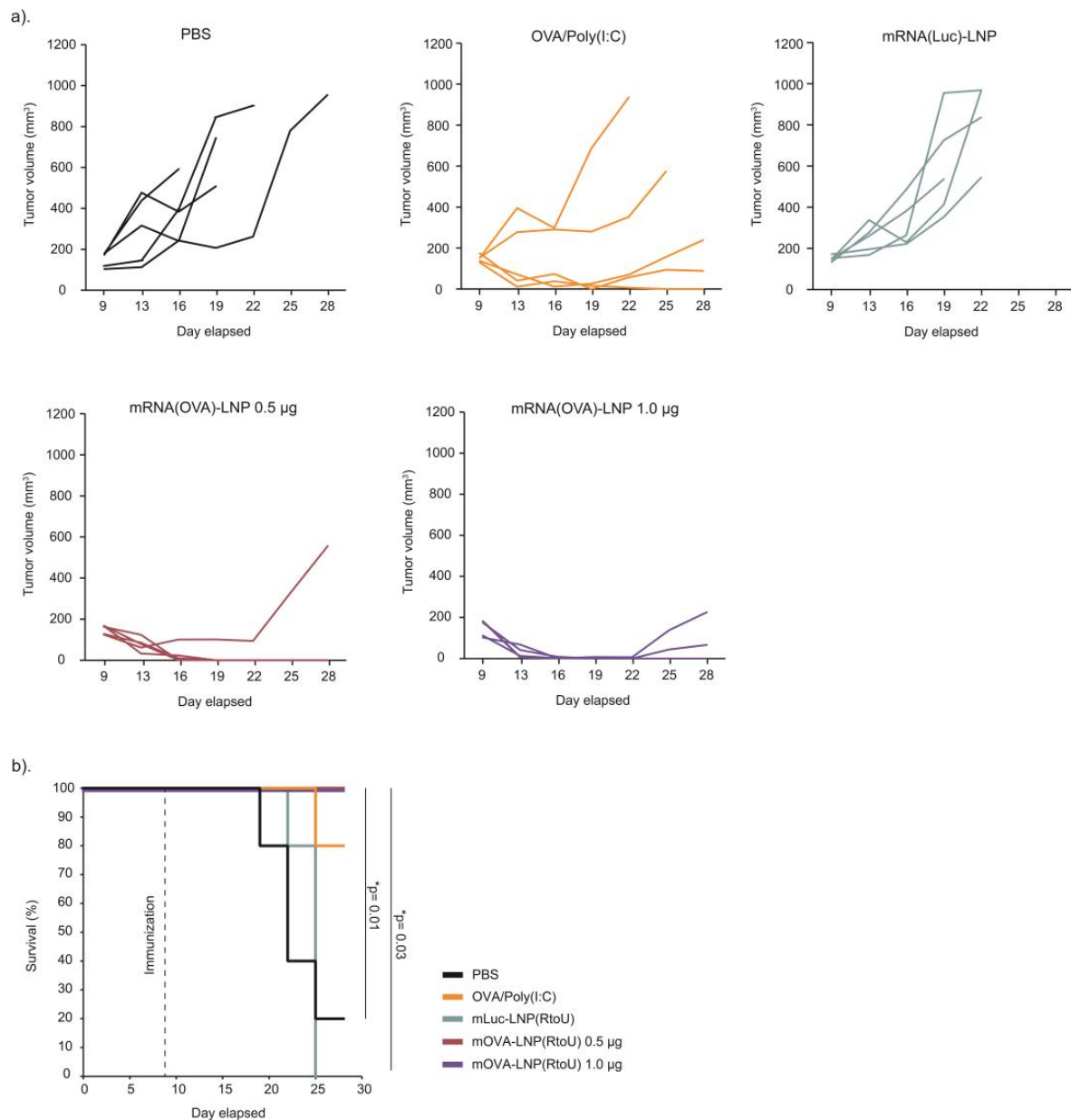


Figure 7. Therapeutic anti-tumor response of $\text{LNPs}_{\text{ssPalmE-Phe}}(\text{RtoU})$. The antitumor response of $\text{LNPs}_{\text{ssPalmE-Phe}}(\text{RtoU})$ against E.G7-OVA tumor-bearing mice was evaluated. E.G7-OVA cells (8.0×10^5 cells/40 μL) were s.c. inoculated on the left flank of C57BL/6J mice ($n = 5$). After the tumor grew to $\geq 100 \text{ mm}^3$ in volume, mOVA- $\text{LNP}_{\text{ssPalmE-Phe}}(\text{RtoU})$ was administered (s.c.) at a dose of 0.5 or 1.0 μg of mRNA. The tumor volumes were monitored in 3-day intervals from day 9 to day 25. The end point was set at a tumor volume of 1000 mm^3 . (a) Individual tumor growth in each treatment group. (b) The overall survival of tumor-bearing mice was determined through a Kaplan–Meier analysis. Significant differences were found between mOVA-LNPs(RtoU), 0.5 μg and 1.0 μg , with PBS (* $p = 0.01$) and mLuc-LNPs(RtoU) (* $p = 0.03$).

4. Discussion

The ionizable lipid ssPalmE-Phe-P4C2 was designed so as to combine two important functions for an RNA vaccine: a vitamin E scaffold for immune activation and a phenyl ester for self-degradability, respectively. Regarding Vitamin E, it has been used as a key component in AS03, a squalene-based oil-in-water emulsion adjuvant that is used in vaccines against the avian influenza virus [23–25]. It has been reported that the vitamin E in the AS03-adjuvanted vaccine modulates the production of cytokines and chemokines such as CCL2, CCL3, IL-6, CSF3, and CXCL1 and promotes antigen-loading monocytes as well as the recruitment of granulocytes [26]. The ssPalm with vitamin E scaffolds (ssPalmE) was initially developed to deliver nucleic acids to the liver; the delivery of siRNA by LNPs_{ssPalmE} demonstrated gene knockdown efficiency and extensive liver accumulation compared to other ssPalms with myristic acid or retinoic acid [15]. The molecular tuning of the ssPalmE through attaching tertiary amines to a piperazine ring resulted in the formation of the second-generation ssPalmE-P4C2, which demonstrated an efficient endosomal escape activity, which contributed to the improved gene knockdown efficiency [15,17]. However, LNPs prepared with ssPalmE derivatives (with piperazine as the tertiary amine structure) triggered severe inflammatory responses that involved the production of pro-inflammatory cytokines (IL6, TNF α), the intracellular DNA-sensor-related cytokine (IL-1 β), and interferon (IFN β) when they were combined with plasmid DNA. From these observations, we hypothesized that the LNPs formed with the ssPalmE derivative would be applicable for use as an RNA vaccine [16]. It was revealed that the mRNA LNPs_{ssPalmE} acted as both a nucleic acid (mRNA) carrier and as an immune adjuvant by inducing the proliferation of antigen-specific CD8⁺ T cells and their differentiation into effector and memory cells to activate cellular immunity [18]. However, the mechanism concerning the ssPalmE-triggered immune activation is not clear.

Studies have demonstrated the capability of vaccines and an adjuvant to induce immunogenicity by stimulating the damage-associated molecular patterns (DAMPs) pathway [27,28]. Cellular stressors or cell death signaling can trigger the release of DAMPs that are then recognized by other cells via pattern recognition receptors (PRRs). This interaction will result in immunogenic reactions, such as the upregulation of the chemokine/cytokines involved in immune responses. Renowned vaccine adjuvants such as Alum, AS03, and HP- β -cyclodextrin are known to induce the release of DAMP signals, which stimulates and enhances the immunogenicity of vaccines [27]. Our previous study also reported the detection of dsDNA at the injection site (skin) upon LNP_{ssPalmE} administration. This finding suggests that the adjuvant effect of LNPs_{ssPalmE-Phe} (RtoU) could also be dependent on this DAMP pathway [18]. Further investigation is required into the cells and molecules involved in this response. It is noteworthy that the use of a simple combination of α -tocopherol and α -tocopherol succinates as a component of poorly immune-stimulative LNPs (formed with a myristic acid-scaffold ssPalm) did not enhance cytokine production [18]. The covalent linkage of α -tocopherol and a tertiary amine into a single molecular structure and/or the dimerization of α -tocopherol could be key factors in the adjuvant effect. Thus, it is plausible that the action of the LNPs_{ssPalmE} involves a mechanism that differs from that of AS03.

The other molecular design integrated in ssPalmE-P4C2 is the introduction of a phenyl ester. The degradability of ionizable lipids in the body has been investigated as a strategy for reducing adverse side effects caused by the accumulation of lipid-like materials. The introduction of ester bonds and/or disulfide bonds is one of the common strategies for achieving the biodegradation of an LNP [15]. It was reported that the combination of disulfide bonds and a phenyl ester moiety synergistically enhances the transfection activity of mRNA by inducing an intraparticle self-degradation that occurs within the limited intraparticle spaces. This reaction induces the release of the nucleic acid cargo [17]. Actually, an siRNA-LNP that contains an oleic-acid-based self-degradable ssPalm (ssPalmO-Phe-P4C2) showed an ED₅₀ of 0.0044 mg/kg siRNA in the liver when administered via an i.v. injection [15]. Comparing the knockdown activity of ssPalmE-P4C2 with that of ssPalmO-Phe-P4C2, the findings suggested that the efficiencies of nucleic acid delivery for

these two materials were significantly different. From this finding, we concluded that the combination of vitamin E scaffolds and phenyl esters is a strategy that can satisfy both immunostimulatory properties and nucleic acid delivery efficiency. The improvement in the luciferase activity and CTL activity of LNP_{ssPalmE-Phe} over LNP_{ssPalmE} suggested that the release of mRNA promoted by self-degradability is an important factor for improving the efficacy of an RNA vaccine. The LNP_{ssPalmE-Phe}(RtoU) also demonstrated strong CTL activity and a significant suppression of E.G7-OVA tumor growth (Figure 7). These observations suggest that ssPalmE-Phe-P4C2 would be a reasonable candidate for use in designing an RNA vaccine that focuses on the activation of cellular immunity.

It is noteworthy that the mRNAs used in this study were unmodified/unpurified. However, in the case of ionizable lipids with vitamin E scaffolds, the hydrophobic scaffold contributed significantly to the adjuvant activity of the LNPs [18]. The contribution of mRNA to the adjuvant activity was negligible. Therefore, ssPalmE-Phe-P4C2, rather than the IVT-mRNA, is considered to be responsible for the immunostimulatory properties of the mRNA-LNPs [18]. Since the improvement in the quality of mRNA can positively affect the vaccine activity of an RNA vaccine [29], the combination of chemically modified and purified mRNA with LNP_{ssPalmE-Phe}(RtoU) would be a potent strategy for the further development of cancer vaccines.

The ready-to-use (RtoU) formulation, a freeze-drying-based preparation method of mRNA-LNPs, was then applied to the LNP_{ssPalmE-Phe} to further develop them as a convenient nucleic acid carrier. Freeze-drying has been extensively used in pharmaceutical industries to improve the stability and shelf life of drug products [19,30,31]. However, the stresses associated with freezing and drying can damage biomolecules unless an appropriate cryoprotectant and lipid composition are used [32]. In this study, the successful application of an RtoU formulation produced mRNA-LNPs that allow for the post-encapsulation of the desired nucleic acids to be achieved via simple rehydration and incubation. The LNP_{ssPalmE-Phe}(RtoU) offers handling practicality and a high rate of encapsulation (>90%) with a minimum loss of nucleic acids. The limitation of the LNP_{ssPalmE-Phe}(RtoU) formulation involves the concentration (1.0 µg mRNA/200 µL) and scale (1.0 µg mRNA/vial) of the resultant mRNA-LNPs. Although this is sufficient for the vaccine experiment in mice, this point should be improved from the viewpoint of other applications.

Sucrose acts as a cryoprotectant, which helps to maintain the stability and integrity of LNPs during the freeze-drying process. The Pfizer/BioNTech and Moderna COVID-19 mRNA vaccines both used sucrose as a cryoprotectant to protect and stabilize the LNPs while in a deep-frozen state (−80 °C) during distribution [33–36]. The Food and Drug Administration authorized the most recent formula of the Pfizer/BioNTech and Moderna COVID-19 mRNA vaccines (2023–2024 Formula), which corresponds to the Omicron variant XBB.1.5 of SARS-CoV-2. In this recent formula, the Pfizer/BioNTech COVID-19 mRNA vaccine used 31 mg of sucrose in each 0.3 mL dose (103.3 mg/mL) [37]; meanwhile, the Moderna COVID-19 mRNA vaccine used 21.8 mg of sucrose in each 0.25 mL dose (87.2 mg/mL) [38]. Compared to a frozen vaccine product, such as the COVID-19 mRNA vaccines, a much higher sucrose concentration is needed to stabilize a lyophilized vaccine product. It was mentioned that sugar molecules replace the water between the hydrophilic heads of phospholipids during lyophilization, thus lowering the phase transition temperature and preventing a gel-to-liquid phase transition [31]. It was also suggested that sugar forms glass matrixes, trapping phospholipids upon the removal of water, which prevents lipid aggregation and damage by ice crystals [31,39]. In this study, sucrose was used as a cryoprotectant for the LNP_{ssPalmE-Phe}(RtoU) following a previously reported procedure [20,40]. The dent or shrinkage appearance of the LNP_{ssPalmE-Phe}(RtoU) is probably related to the formulation process, in which the secondary drying process was apparently too rapid [22]. The amount of sucrose and/or the freeze-drying process should be optimized for each application. In our experiments, the dent appearance of the lyophilized product had no effect on the product's quality. This is consistent with the general notion that a dent appearance is acceptable [22]. The pH of the buffer is another

important factor in preparing an LNP, especially for the post-encapsulation of mRNA. The electrostatic interaction between ionizable lipids and nucleic acids is probably the main driving force in the post-encapsulation process [20]. It should be noted here that the buffer pH (5.0) together with a high concentration of sucrose (320 mg/mL) produced preferable particle properties (Table 2) and a high immune activation activity (Figure 5).

The established RtoU formulation (ssPalm/helper lipid/cholesterol = 52.5/7.5/40) [20] was found to be the most suitable lipid composition for the LNP_{ssPalmE-Phe}, which demonstrated stronger immune activation activity compared to the other formulations (Figure 6). This observation is closely related to the cholesterol composition. Cholesterol is known to have the ability to provide cryoprotection for LNPs during freeze-drying by maintaining the stability of lipid formation and preventing the risk of leakage of contents [41,42]. In addition, it was revealed that a cholesterol content of at least 40% in the LNP_{ssPalm} was essential for achieving a high transfection activity of the phenyl-type ionizable lipid [17]. The ONPATTRO[®] or Patisiran (Alnylam Pharmaceutical, Cambridge, MA, USA) also utilizes a cholesterol content > 30% (38.5%) in its LNP formulation for siRNA delivery [33]. Moreover, the current COVID-19 mRNA vaccines by Pfizer/BioNTech and Moderna also utilize a cholesterol content >30% in their LNP formulation, with 42.7% and 38.5% cholesterol, respectively [33]. Although the exact composition of cholesterol varies depending on the type of ionizable lipid and its delivery purpose, a cholesterol content of at least around 40% in the LNP formulation might be important in terms of exerting its mRNA delivery efficiency. The limitation of the LNP(RtoU) formulation is the concentration (1.0 µg/200 µL) and scale (1.0 µ/vial) of the resultant mRNA-LNPs. Although this is enough for the vaccine experiment in mice, this point should be improved from the viewpoint of other applications.

Phospholipids are also included as helper lipids to provide particle stability and delivery efficiency [43]. DOPE is a cone-shaped lipid with high fusogenic activity, while DOPC functions to stabilize the LNPs through its overall cylindrical shape. Both lipids were used to form the microfluidic-mixer-type (Figure 3) or the RtoU-type (Figure 4) LNP_{ssPalmE-Phe}. As a result, the use of DOPE was revealed to be important for achieving higher activity of cytotoxic T cells. The findings indicated that the CTL activity of the LNP_{ssPalmE-Phe}(RtoU) tended to increase when the DOPE ratio was reduced. However, the complete removal of the helper lipid was shown to be detrimental to the CTL activity of the LNP_{ssPalmE-Phe}(RtoU). This indicates there is a delicate balance between the ionizable lipid, the helper lipid, and the amount of cholesterol needed to achieve an optimum lipid composition. When the cholesterol ratio was fixed, the DOPE ratio was accompanied by an increase in the ssPalmE-Phe-P4C2 ratio. Thus, the amount of ionizable lipid holds priority in the lipid composition, which determines the immune activation activity of the LNP_{ssPalmE-Phe}(RtoU).

5. Conclusions

Ready-to-use-type LNP_{ssPalmE-Phe} offer a convenient form of an mRNA-based vaccine carrier. The LNP_{ssPalmE-Phe}(RtoU) were capable of post-encapsulating the intended mRNA antigens through a simple rehydration/incubation step. The efficacy of the LNP_{ssPalmE-Phe}(RtoU) to significantly suppress tumor progression indicated their usefulness in cancer vaccine development. Therefore, this RtoU technology would be suitable for easily screening novel antigens/neo-antigens and/or confirming a proof-of-concept as to whether the candidate gene actually functions as an antigen for cancer therapy.

Supplementary Materials: The following supporting information can be downloaded at <https://www.mdpi.com/article/10.3390/pharmaceutics15122702/s1>: Table S1: Detailed list of materials used in the study; Table S2: Physicochemical properties of LNP_{ssPalmE-Phe}(RtoU) lipid composition screening; Figure S1: CTL activity of LNP_{ssPalmE-Phe}(RtoU) prepared with or without ultrafiltration; Figure S2: Freeze-dried appearance of LNP_{ssPalmE-Phe}(RtoU); and Figure S3: CTL activity of LNP_{ssPalmE-Phe}(RtoU) prepared with various lipid compositions.

Author Contributions: Conceptualization, J.A., H.T. and H.A.; methodology, S.H. and D.S.; validation, S.T., Y.N., K.T. and Y.S.; formal analysis, J.A. and H.T.; investigation, J.A., R.O., S.H. and D.S.; resources, S.T., Y.N., K.T. and Y.S.; data curation, J.A., R.O., D.S., S.T., Y.N., K.T., H.H. and Y.S.; writing—original draft preparation, J.A. and H.T.; writing—review and editing, R.O., S.H., D.S., S.T., Y.N., K.T., H.H., Y.S. and H.A.; visualization, J.A.; supervision, H.A.; project administration, J.A. and H.A.; funding acquisition, H.T. and H.A. All authors have read and agreed to the published version of the manuscript.

Funding: H. Tanaka was supported by JSPS KAKENHI (18K18377, 21K18035) and the Kato Memorial Bio-science Foundation. H. Akita was supported by a JST CREST grant (grant number JPMJCR17H1), JSPS KAKENHI (grant numbers 20H00657, 21K18320), the Basic Science and Platform Technology Program for Innovative Biological Medicine from the Japan Agency for Medical Research and Development (AMED) under grant number JP21gm1610006, and the Canon Foundation Research Grant Program. H. Tanaka and H. Akita were funded by NOF CORPORATION as joint research.

Institutional Review Board Statement: Protocols for the animal experiments were reviewed and approved by the Chiba University Animal Care Committee in accordance with the “Guide for Care and Use of Laboratory Animals” (No. 4-175).

Informed Consent Statement: Not applicable.

Data Availability Statement: The data presented in this study are available on request from the corresponding author.

Acknowledgments: The authors wish to thank Milton S Feather for his helpful advice in writing the English manuscript.

Conflicts of Interest: H. Tanaka, Y. Nakai, K. Tange, and H. Akita are the inventors of a patent pending (WO2019/188867) on the ssPalm chemicals. This research was conducted as a joint research between Tohoku University, Chiba University, and the NOF CORPORATION.

References

1. Liu, M.A. A Comparison of Plasmid DNA and mRNA as Vaccine Technologies. *Vaccines* **2019**, *7*, 37. [[CrossRef](#)] [[PubMed](#)]
2. Zhang, C.; Maruggi, G.; Shan, H.; Li, J. Advances in mRNA Vaccines for Infectious Diseases. *Front. Immunol.* **2019**, *10*, 594. [[CrossRef](#)] [[PubMed](#)]
3. Pardi, N.; Hogan, M.J.; Porter, F.W.; Weissman, D. mRNA Vaccines—A New Era in Vaccinology. *Nat. Rev. Drug Discov.* **2018**, *17*, 261–279. [[CrossRef](#)] [[PubMed](#)]
4. Qin, F.; Xia, F.; Chen, H.; Cui, B.; Feng, Y.; Zhang, P.; Chen, J.; Luo, M. A Guide to Nucleic Acid Vaccines in the Prevention and Treatment of Infectious Diseases and Cancers: From Basic Principles to Current Applications. *Front. Cell Dev. Biol.* **2021**, *9*, 830. [[CrossRef](#)] [[PubMed](#)]
5. Urits, I.; Swanson, D.; Swett, M.C.; Patel, A.; Bernardino, K.; Amgalan, A.; Berger, A.A.; Kassem, H.; Kaye, A.; Viswanath, O. A Review of Patisiran (ONPATRO[®]) for the Treatment of Polyneuropathy in People with Hereditary Transthyretin Amyloidosis. *Neurol. Ther.* **2020**, *9*, 301–315. [[CrossRef](#)] [[PubMed](#)]
6. Adams, D.; Polydefkis, M.; González-Duarte, A.; Wixner, J.; Kristen, A.V.; Schmidt, H.H.; Berk, J.L.; Losada López, I.A.; Dispenzieri, A.; Quan, D.; et al. Long-Term Safety and Efficacy of Patisiran for Hereditary Transthyretin-Mediated Amyloidosis with Polyneuropathy: 12-Month Results of an Open-Label Extension Study. *Lancet Neurol.* **2021**, *20*, 49–59. [[CrossRef](#)]
7. Maurer, M.S.; Kale, P.; Fontana, M.; Berk, J.L.; Grogan, M.; Gustafsson, F.; Hung, R.R.; Gottlieb, R.L.; Damy, T.; González-Duarte, A.; et al. Patisiran Treatment in Patients with Transthyretin Cardiac Amyloidosis. *N. Engl. J. Med.* **2023**, *389*, 1553–1565. [[CrossRef](#)]
8. Adams, D.; Gonzalez-Duarte, A.; O’Riordan, W.D.; Yang, C.-C.; Ueda, M.; Kristen, A.V.; Tournev, I.; Schmidt, H.H.; Coelho, T.; Berk, J.L.; et al. Patisiran, an RNAi Therapeutic, for Hereditary Transthyretin Amyloidosis. *N. Engl. J. Med.* **2018**, *379*, 11–21. [[CrossRef](#)]
9. Akinc, A.; Maier, M.A.; Manoharan, M.; Fitzgerald, K.; Jayaraman, M.; Barros, S.; Ansell, S.; Du, X.; Hope, M.J.; Madden, T.D.; et al. The Onpattro Story and the Clinical Translation of Nanomedicines Containing Nucleic Acid-Based Drugs. *Nat. Nanotechnol.* **2019**, *14*, 1084–1087. [[CrossRef](#)]
10. Polack, F.P.; Thomas, S.J.; Kitchin, N.; Absalon, J.; Gurtman, A.; Lockhart, S.; Perez, J.L.; Pérez Marc, G.; Moreira, E.D.; Zerbini, C.; et al. Safety and Efficacy of the BNT162b2 mRNA Covid-19 Vaccine. *N. Engl. J. Med.* **2020**, *383*, 2603–2615. [[CrossRef](#)]
11. Walsh, E.E.; Frenck, R.W.; Falsey, A.R.; Kitchin, N.; Absalon, J.; Gurtman, A.; Lockhart, S.; Neuzil, K.; Mulligan, M.J.; Bailey, R.; et al. Safety and Immunogenicity of Two RNA-Based Covid-19 Vaccine Candidates. *N. Engl. J. Med.* **2020**, *383*, 2439–2450. [[CrossRef](#)] [[PubMed](#)]
12. Jackson, L.A.; Anderson, E.J.; Roupael, N.G.; Roberts, P.C.; Makhene, M.; Coler, R.N.; McCullough, M.P.; Chappell, J.D.; Denison, M.R.; Stevens, L.J.; et al. An mRNA Vaccine against SARS-CoV-2—Preliminary Report. *N. Engl. J. Med.* **2020**, *383*, 1920–1931. [[CrossRef](#)] [[PubMed](#)]

13. El Sahly, H.M.; Baden, L.R.; Essink, B.; Doblecki-Lewis, S.; Martin, J.M.; Anderson, E.J.; Campbell, T.B.; Clark, J.; Jackson, L.A.; Fichtenbaum, C.J.; et al. Efficacy of the mRNA-1273 SARS-CoV-2 Vaccine at Completion of Blinded Phase. *N. Engl. J. Med.* **2021**, *385*, 1774–1785. [[CrossRef](#)] [[PubMed](#)]
14. Watson, O.J.; Barnsley, G.; Toor, J.; Hogan, A.B.; Winskill, P.; Ghani, A.C. Global Impact of the First Year of COVID-19 Vaccination: A Mathematical Modelling Study. *Lancet Infect. Dis.* **2022**, *22*, 1293–1302. [[CrossRef](#)] [[PubMed](#)]
15. Tanaka, H.; Sakurai, Y.; Anindita, J.; Akita, H. Development of Lipid-like Materials for RNA Delivery Based on Intracellular Environment-Responsive Membrane Destabilization and Spontaneous Collapse. *Adv. Drug Deliv. Rev.* **2020**, *154–155*, 210–226. [[CrossRef](#)] [[PubMed](#)]
16. Tateshita, N.; Miura, N.; Tanaka, H.; Masuda, T.; Ohtsuki, S.; Tange, K.; Nakai, Y.; Yoshioka, H.; Akita, H. Development of a Lipoplex-Type mRNA Carrier Composed of an Ionizable Lipid with a Vitamin E Scaffold and the KALA Peptide for Use as an Ex Vivo Dendritic Cell-Based Cancer Vaccine. *J. Control. Release* **2019**, *310*, 36–46. [[CrossRef](#)] [[PubMed](#)]
17. Tanaka, H.; Takahashi, T.; Konishi, M.; Takata, N.; Gomi, M.; Shirane, D.; Miyama, R.; Hagiwara, S.; Yamasaki, Y.; Sakurai, Y.; et al. Self-Degradable Lipid-Like Materials Based on “Hydrolysis Accelerated by the Intra-Particle Enrichment of Reactant (HYPER)” for Messenger RNA Delivery. *Adv. Funct. Mater.* **2020**, *30*, 1910575. [[CrossRef](#)]
18. Oyama, R.; Ishigame, H.; Tanaka, H.; Tateshita, N.; Itazawa, M.; Imai, R.; Nishiumi, N.; Kishikawa, J.; Kato, T.; Anindita, J.; et al. An Ionizable Lipid Material with a Vitamin E Scaffold as an mRNA Vaccine Platform for Efficient Cytotoxic T Cell Responses. *ACS Nano* **2023**, *17*, 18758–18774. [[CrossRef](#)]
19. Lball, R.; Bajaj, P.; Whitehead, K.A. Achieving Long-Term Stability of Lipid Nanoparticles: Examining the Effect of PH, Temperature, and Lyophilization. *Int. J. Nanomed.* **2017**, *12*, 305. [[CrossRef](#)]
20. Tanaka, H.; Hagiwara, S.; Shirane, D.; Yamakawa, T.; Sato, Y.; Matsumoto, C.; Ishizaki, K.; Hishinuma, M.; Chida, K.; Sasaki, K.; et al. Ready-to-Use-Type Lyophilized Lipid Nanoparticle Formulation for the Postencapsulation of Messenger RNA. *ACS Nano* **2023**, *17*, 2588–2601. [[CrossRef](#)]
21. Haeuser, C.; Goldbach, P.; Huwylar, J.; Friess, W.; Allmendinger, A. Excipients for Room Temperature Stable Freeze-Dried Monoclonal Antibody Formulations. *J. Pharm. Sci.* **2020**, *109*, 807–817. [[CrossRef](#)] [[PubMed](#)]
22. Patel, S.M.; Nail, S.L.; Pikal, M.J.; Geidobler, R.; Winter, G.; Hawe, A.; Davagnino, J.; Rambhatla Gupta, S. Lyophilized Drug Product Cake Appearance: What Is Acceptable? *J. Pharm. Sci.* **2017**, *106*, 1706–1721. [[CrossRef](#)] [[PubMed](#)]
23. Howard, L.M.; Goll, J.B.; Jensen, T.L.; Hoek, K.L.; Prasad, N.; Gelber, C.E.; Levy, S.E.; Joyce, S.; Link, A.J.; Buddy Creech, C.; et al. AS03-Adjuvanted H5N1 Avian Influenza Vaccine Modulates Early Innate Immune Signatures in Human Peripheral Blood Mononuclear Cells. *J. Infect. Dis.* **2019**, *219*, 1786–1798. [[CrossRef](#)] [[PubMed](#)]
24. Khurana, S.; Coyle, E.M.; Manischewitz, J.; King, L.R.; Gao, J.; Germain, R.N.; Schwartzberg, P.L.; Tsang, J.S.; Golding, H.; Biancotto, A.; et al. AS03-Adjuvanted H5N1 Vaccine Promotes Antibody Diversity and Affinity Maturation, NAI Titers, Cross-Clade H5N1 Neutralization, but Not H1N1 Cross-Subtype Neutralization. *NPJ Vaccines* **2018**, *3*, 40. [[CrossRef](#)] [[PubMed](#)]
25. Cohet, C.; van der Most, R.; Bauchau, V.; Bekkat-Berkani, R.; Doherty, T.M.; Schuind, A.; Tavares Da Silva, F.; Rappuoli, R.; Garçon, N.; Innis, B.L. Safety of AS03-Adjuvanted Influenza Vaccines: A Review of the Evidence. *Vaccine* **2019**, *37*, 3006–3021. [[CrossRef](#)] [[PubMed](#)]
26. Morel, S.; Didierlaurent, A.; Bourguignon, P.; Delhay, S.; Baras, B.; Jacob, V.; Planty, C.; Elouahabi, A.; Harvengt, P.; Carlsen, H.; et al. Adjuvant System AS03 Containing α -Tocopherol Modulates Innate Immune Response and Leads to Improved Adaptive Immunity. *Vaccine* **2011**, *29*, 2461–2473. [[CrossRef](#)] [[PubMed](#)]
27. Lee, S.M.; Kim, P.; You, J.; Kim, E.H. Role of Damage-Associated Molecular Pattern/Cell Death Pathways in Vaccine-Induced Immunity. *Viruses* **2021**, *13*, 2340. [[CrossRef](#)]
28. Patidar, A.; Selvaraj, S.; Sarode, A.; Chauhan, P.; Chattopadhyay, D.; Saha, B. DAMP-TLR-Cytokine Axis Dictates the Fate of Tumor. *Cytokine* **2018**, *104*, 114–123. [[CrossRef](#)]
29. Bernard, M.-C.; Bazin, E.; Petiot, N.; Lemdani, K.; Commandeur, S.; Verdelet, C.; Margot, S.; Perkov, V.; Ripoll, M.; Garinot, M.; et al. The Impact of Nucleoside Base Modification in mRNA Vaccine Is Influenced by the Chemistry of Its Lipid Nanoparticle Delivery System. *Mol. Ther. Nucleic Acids* **2023**, *32*, 794–806. [[CrossRef](#)]
30. Kasper, J.C.; Winter, G.; Friess, W. Recent Advances and Further Challenges in Lyophilization. *Eur. J. Pharm. Biopharm.* **2013**, *85*, 162–169. [[CrossRef](#)]
31. Chen, C.; Han, D.; Cai, C.; Tang, X. An Overview of Liposome Lyophilization and Its Future Potential. *J. Control. Release* **2010**, *142*, 299–311. [[CrossRef](#)] [[PubMed](#)]
32. Kristensen, D.D.; Lorenson, T.; Bartholomew, K.; Villadiego, S. Can Thermostable Vaccines Help Address Cold-Chain Challenges? Results from Stakeholder Interviews in Six Low- and Middle-Income Countries. *Vaccine* **2016**, *34*, 899–904. [[CrossRef](#)] [[PubMed](#)]
33. Schoenmaker, L.; Witzigmann, D.; Kulkarni, J.A.; Verbeke, R.; Kersten, G.; Jiskoot, W.; Crommelin, D.J.A. mRNA-Lipid Nanoparticle COVID-19 Vaccines: Structure and Stability. *Int. J. Pharm.* **2021**, *601*, 120586. [[CrossRef](#)] [[PubMed](#)]
34. Sahin, U.; Muik, A.; Vogler, I.; Derhovanessian, E.; Kranz, L.M.; Vormehr, M.; Quandt, J.; Bidmon, N.; Ulges, A.; Baum, A.; et al. BNT162b2 Vaccine Induces Neutralizing Antibodies and Poly-Specific T Cells in Humans. *Nature* **2021**, *595*, 572–577. [[CrossRef](#)] [[PubMed](#)]
35. Corbett, K.S.; Edwards, D.K.; Leist, S.R.; Abiona, O.M.; Boyoglu-Barnum, S.; Gillespie, R.A.; Himansu, S.; Schäfer, A.; Ziwawo, C.T.; DiPiazza, A.T.; et al. SARS-CoV-2 mRNA Vaccine Design Enabled by Prototype Pathogen Preparedness. *Nature* **2020**, *586*, 567–571. [[CrossRef](#)] [[PubMed](#)]

36. Urru, S.A.M.; Maines, E.; Campomori, A.; Soffiati, M. Safety of Sars-Cov-2 Vaccines Administration for Adult Patients with Hereditary Fructose Intolerance. *Hum. Vaccin. Immunother.* **2021**, *17*, 4112. [[CrossRef](#)]
37. U.S. Food & Drug Administration Pfizer-BioNTech COVID-19 Vaccine. Available online: <https://www.fda.gov/vaccines-blood-biologics/coronavirus-covid-19-cber-regulated-biologics/pfizer-biontech-covid-19-vaccine> (accessed on 12 September 2023).
38. U.S. Food & Drug Administration Moderna COVID-19 Vaccine. Available online: <https://www.fda.gov/vaccines-blood-biologics/coronavirus-covid-19-cber-regulated-biologics/moderna-covid-19-vaccine> (accessed on 12 September 2023).
39. Wolfe, J.; Bryant, G. Freezing, Drying, and/or Vitrification of Membrane–Solute–Water Systems. *Cryobiology* **1999**, *39*, 103–129. [[CrossRef](#)]
40. Shirane, D.; Tanaka, H.; Nakai, Y.; Yoshioka, H.; Akita, H. Development of an Alcohol Dilution–Lyophilization Method for Preparing Lipid Nanoparticles Containing Encapsulated siRNA. *Biol. Pharm. Bull.* **2018**, *41*, 1291–1294. [[CrossRef](#)]
41. Ohtake, S.; Schebor, C.; Palecek, S.P.; De Pablo, J.J. Phase Behavior of Freeze-Dried Phospholipid–Cholesterol Mixtures Stabilized with Trehalose. *Biochim. Et Biophys. Acta BBA Biomembr.* **2005**, *1713*, 57–64. [[CrossRef](#)]
42. Franzé, S.; Selmin, F.; Samaritani, E.; Minghetti, P.; Cilurzo, F. Lyophilization of Liposomal Formulations: Still Necessary, Still Challenging. *Pharmaceutics* **2018**, *10*, 139. [[CrossRef](#)]
43. Cheng, X.; Lee, R.J. The Role of Helper Lipids in Lipid Nanoparticles (LNPs) Designed for Oligonucleotide Delivery. *Adv. Drug Deliv. Rev.* **2016**, *99*, 129–137. [[CrossRef](#)] [[PubMed](#)]

Disclaimer/Publisher’s Note: The statements, opinions and data contained in all publications are solely those of the individual author(s) and contributor(s) and not of MDPI and/or the editor(s). MDPI and/or the editor(s) disclaim responsibility for any injury to people or property resulting from any ideas, methods, instructions or products referred to in the content.